# In vivo far-red luminescence imaging of a biomarker based on BRET from *Cypridina* bioluminescence to an organic dye

**Chun Wu[a], Kazuhiro Mino[b], Hidetoshi Akimoto[b], Makiko Kawabata[c], Koji Nakamura[c], Michitaka Ozaki[b], and Yoshihiro Ohmiya[a,b,d,1]**

[a]Research Institute for Cell Engineering, National Institute of Advanced Industrial Science and Technology, 1-8-31 Midorigaoka, Ikeda 563-8577, Japan; [b]Graduate School of Medicine, Hokkaido University, Kita-15, Nishi-7, Kita-ku, Sapporo 060-8638, Japan; [c]LivTech, Inc, 907 Nogawa, Miyamae-ku, Kawasaki 216-0001, Japan; and [d]Research Institute for Genome-based Biofactory, National Institute of Advanced Industrial Science and Technology, 2-17-2-1 Tsukisamu-Higashi, Sapporo 062-8517, Japan

Communicated by J. Woodland Hastings, Harvard University, Cambridge, MA, July 30, 2009 (received for review October 23, 2008)

**We aimed to develop a far-red luminescence imaging technology for visualization of disease specific antigens on cell surfaces in a living body. First, we conjugated a far-red fluorescent indocyanine derivative to biotinylated *Cypridina* luciferase. This conjugate produced a bimodal spectrum that has long-wavelength bioluminescence emission in the far-red region as a result of bioluminescence resonance energy transfer. To generate a far-red luminescent probe with targeting and imaging capabilities of tumors, we then linked this conjugate to an anti-human Dlk-1 monoclonal antibody via the biotin-avidin interaction. This far-red luminescent probe enabled us to obtain high-resolution microscopic images of live, Dlk-1-expressing Huh-7 cells without an external light source, and to monitor the accumulation of this probe in tumor-bearing mice. Thus this far-red luminescent probe is a convenient analytical tool for the evaluations of monoclonal antibody localization in a living body.**

*Cypridina* luciferase | far-red luminescent probe | luciferin | tumor

An increasing number of monoclonal antibodies have been used to target antigens on cancer cells for clinical diagnosis and therapy, based on the fact that some antigens expressed on cancer cells surface reflect malignant behaviors invasion, metastasis, and neo-vascularization (1–5). Molecular imaging of antibodies in the whole body will enable us to prescribe the appropriate antibody therapy in terms of dose and the timing of administration. Fluorescence imaging (FLI) and bioluminescence imaging (BLI) have played an important role in molecular imaging in small animals (6–8). Photon detection is affordable and easy to use compared with radioisotope imaging. BLI is achieved with a luciferin-luciferase reaction in the presence of molecular oxygen. However, most bioluminescence spectra are in the visible region, overlapping with the absorption spectrum of hemoglobin, attenuating the bioluminescence intensity in live animals. Recently, a "self-illuminating quantum dot probe" was developed to improve the light penetration based on bioluminescence resonance energy transfer (BRET) between the bioluminescence of *Renilla* luciferase and quantum dots (9). The multivalent conjugation of *Renilla* luciferase to single dots allowed for highly efficient BRET between luciferase and quantum dots. However, the large size of the conjugate may cause problems in metabolism and localization in vivo (10).

BRET is a natural phenomenon observed in marine organisms. Green fluorescent protein, for example, is a well-known energy acceptor in the bioluminescence of *Renilla* luciferase and aequorin. BRET between the bioluminescence of *Renilla* luciferase and green fluorescent protein mutants has been used to study protein interactions (11). Recently several far-red fluorescent protein variants showing emission maxima around 650 nm were developed for in vivo imaging (12), but have not been well characterized as energy acceptors for BRET systems. On the other hand, the organic dyes indocyanine and its derivatives have molecular weights less than 1,200 Da, they produce far-red fluorescence and are widely used for in vivo imaging applications (13). Luciferase conjugated to such organic dyes is expected to create possibilities for in vivo applications.

*Cypridina* luciferase (CLuc) catalyzes the oxidation of *Cypridina* luciferin to yield light emission peaking at 460 nm (14). The luciferase genes from both the so-called sea fireflies *Cypridina* (*Vargula*) *hilgendorfii* and *C. noctiluca* have been cloned (15, 16); we used the latter. The 62-kDa CLuc has some unique properties as a bioluminescent enzyme (17). The secreted protein contains 17 disulfide bond pairs and is highly stable under physiological conditions. Its turnover rate (1,400 luciferin molecules per minute) is the highest among known luciferases (18). Recently we have established a method for the synthesis of the substrate, and have expressed the recombinant CLuc in yeast and applied it to ELISA (19, 20).

In the present study, we conjugated a far-red fluorescent indocyanine derivative to biotinylated CLuc via glycol-chains and named this far-red bioluminescent protein "FBP." A monoclonal antibody against human Delta-like protein (Dlk-1), one of the embryonic antigens expressed on the surface of many cancer cells, was then produced (21–25). Using anti-Dlk-1 monoclonal antibody linked to FBP via biotin-avidin interaction, we achieved bioluminescence imaging of cancer cells in vivo as well as in vitro.

## Results

We designed FBP based on BRET (Fig. 1*A*). To obtain biotinylated CLuc (*SI Text*), we attached an Avi-Tag consisting of a 16-residue peptide SGLNDIFEAQKIEWHE to the C terminus of CLuc (26). We then conjugated biotinylated CLuc with the indocyanine derivative HiLyte Fluor™ 647 hydrazide via the glycol-chains of CLuc. The band of FBP on SDS/PAGE was shifted to high molecular weight compared with that of biotinylated CLuc (Fig. 1*B*, lanes 1 and 2). The average substitution was estimated to be two dyes per CLuc molecule from the UV absorption spectrum.

FBP showed a bimodal bioluminescence spectrum, attributable to intra-molecular BRET, having emission peaks at 460 nm and at 675 nm. To investigate the possible effect of pH and ion concentration, we measured bioluminescence spectra under different conditions. No appreciable change was observed (Fig.

Author contributions: C.W., M.O., and Y.O. designed research; C.W., K.M., and H.A. performed research; C.W., M.K., and K.N. contributed new reagents/analytic tools; C.W., K.M., H.A., M.O., and Y.O. analyzed data; and C.W. and Y.O. wrote the paper.

The authors declare no conflict of interest.

Freely available online through the PNAS open access option.

[1]To whom correspondence should be addressed. E-mail: y-ohmiya@aist.go.jp.

This article contains supporting information online at www.pnas.org/cgi/content/full/0908594106/DCSupplemental.

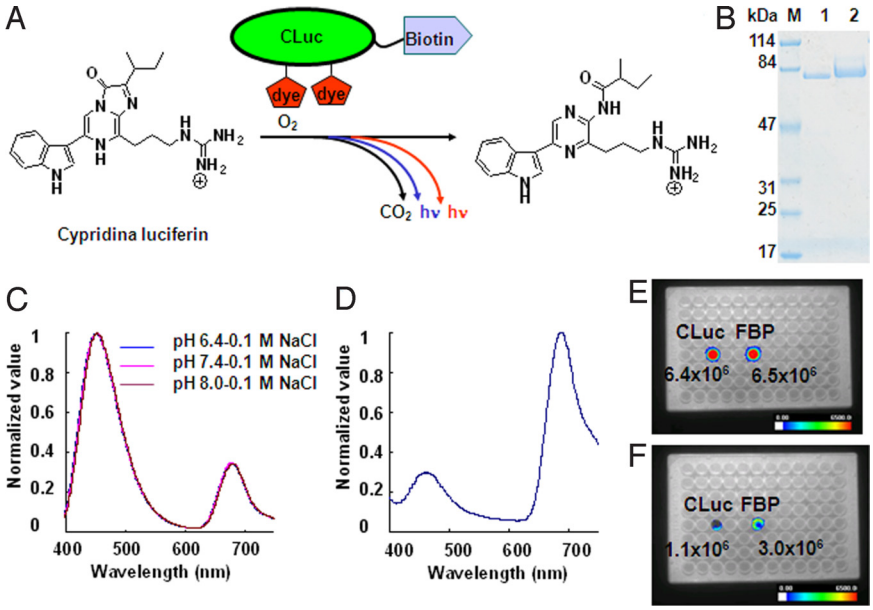


**Fig. 1.** (*A*) Schematic of FBP and its bioluminescence reaction. (*B*) SDS/PAGE of biotinylated CLuc (lane 1) and FBP (lane 2). (*C*) Bioluminescence spectra of FBP measured in different pH buffer solutions containing 0.1 M NaCl. Curves all superimpose. (*D*) Bioluminescence spectrum of FBP in blood. (*E*) Relative light intensity of FBP or CLuc in buffer. (*F*) Relative light intensity of FBP or CLuc in blood.

1*C* and Fig. S1), indicating that the BRET signal was constant under different physiological conditions. To examine whether the BRET signal could be detected in vivo, we measured the bioluminescence spectrum of FBP in mouse blood (Fig. 1*D*). The far-red emission peak was dominant in the bioluminescence spectrum. Furthermore, to compare light intensity of FBP and CLuc under various conditions, we measured these probes in buffer as well as in blood with a commercial CCD imaging system. We found the light intensity of FBP was almost the same as that of CLuc in buffer (Fig. 1*E*), whereas the light intensity of FBP in blood was three-times higher than that of CLuc (Fig. 1*F*). These results suggested that FBP is suitable for in vivo imaging in live animals.

Dlk-1 is one of the embryonic antigens expressed on the surface of many cancer cells. It is highly expressed in fetal tissues including liver, but is undetectable in adult liver (23). To obtain a monoclonal antibody against Dlk-1, we prepared a human embryonic kidney cell line (HEK293 cells) stably expressing Dlk-1-antigen (HEK293-Dlk-1). Mice (BALB/c) were immunized with HEK293-Dlk-1cells or with the expression vector that encodes full-length Dlk-1 cDNA. An anti-human Dlk-1 monoclonal antibody (DI-2–20) was screened by ELISA and flow cytometry. Immunocytochemical analyses showed that the anti-human Dlk-1 monoclonal antibody detected Dlk-1 antigen on Dlk-1-positive human hepato-cellular carcinoma cell line (Huh-7 cells) (Fig. 2*A*). In contrast, no green fluorescence signal was found on the surface of Dlk-1-negative Huh-7 cells (Fig. 2*B*). Western blot analyses clearly indicated the exclusive expression of Dlk-1 antigen on Dlk-1-positive Huh-7 cells (Fig. 2*C*).

After the antibody was conjugated to maleimide-activated avidin, we loaded the reaction mixture on a size-exclusion column (Fig. 3*A*). The eluted fractions were subjected to a bioluminescence ELISA using FBP and anti-mouse IgG coating plate. A high molecular weight protein of approximately 500 kDa showed strong bioluminescence (Fig. 3*B*). To reduce the size of the antibody and avidin conjugate, we treated the antibody with 2-mercaptoethylamine, a mild reducing agent that can selectively cleave hinge-region disulfide bonds between the heavy chains of antibody molecules. The two functional half antibodies were then conjugated to maleimide-activated avidin and purified on a size-exclusion column (Fig. 3*C*); the reduced antibody-avidin conjugate of approximately 200 kDa was collected (Fig. 3*D*).

To evaluate the capabilities of the far-red luminescent probe, which we now call FBP-IgG, consisting of FBP and avidin-bound antibody (Fig. 4*A*), we performed microscopic BLI. After incubating the conjugate with Dlk-1-positive or Dlk-1-negative Huh-7 cells cultured in a dish, a strong bioluminescence signal was observed from Dlk-1-positive Huh-7 cells, but not from Dlk-1-negative Huh-7 cells (Fig. 4 *B* and *C*). For comparison, we similarly prepared a probe CLuc-IgG by mixing biotin-CLuc with avidin-bound reduced anti-Dlk IgG.

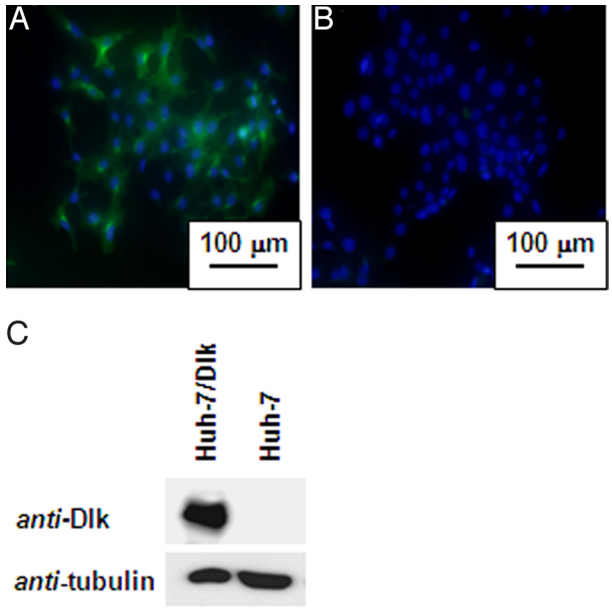


**Fig. 2.** Dlk-1-positive Huh-7 cells. (*A* and *B*) Fluorescence micrographs of Dlk-positive Huh-7/Dlk-1 cells and Huh-7 cells. Hoechst33342 and FITC were used for nuclear staining (blue) and Dlk-1 staining (green), respectively. (*C*) Western blot analyses of Dlk-1-positive and Dlk-1-negative Huh-7 cells.

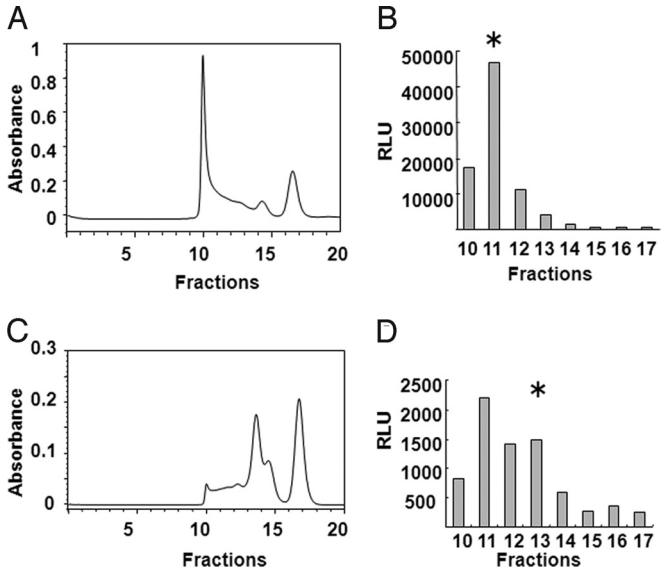


**Fig. 3.** Antibodies linked to avidin. (*A*) Purification of avidin-bound antibody by gel filtration column chromatography on TSK gel G3000SW column. (*B*) Bioluminescence ELISA was used to detect antibody-avidin conjugates; asterisk represents collected fraction. (*C*) Purification of reduced antibody-avidin by gel filtration column chromatography. (*D*) Bioluminescent ELISA was used to detect reduced antibody-avidin conjugates; asterisk represents collected fraction. RLU, relative luminescence unit.

We developed several tumor-bearing nude mice xenografted with Dlk-1-positive Huh-7 cells (Fig. 5 *A* and *B* and Fig. S2 *A* and *B*). At 24 h postinjection of CLuc-IgG (upper panels) or FBP-IgG (lower panels), the mice were injected with a solution of *Cypridina* luciferin, and 5–10 min later, BLI were obtained using a commercial CCD imaging system. The images (Fig. 5 *C* and *D*) showed that both Cluc-IgG and FBP-IgG probes were visible at the tumor site, with that from FBP-IgG two fold higher than that of CLuc-IgG, and the signal to noise ratio also improved. To determine if BRET occurs in these live animals, we measured BLI in the presence of the 570 nm long pass filter. The signal from FBP at the tumor site (Fig. 5*F*) was significantly higher than that of CLuc (Fig. 5*E*), showing that the BRET system was active.

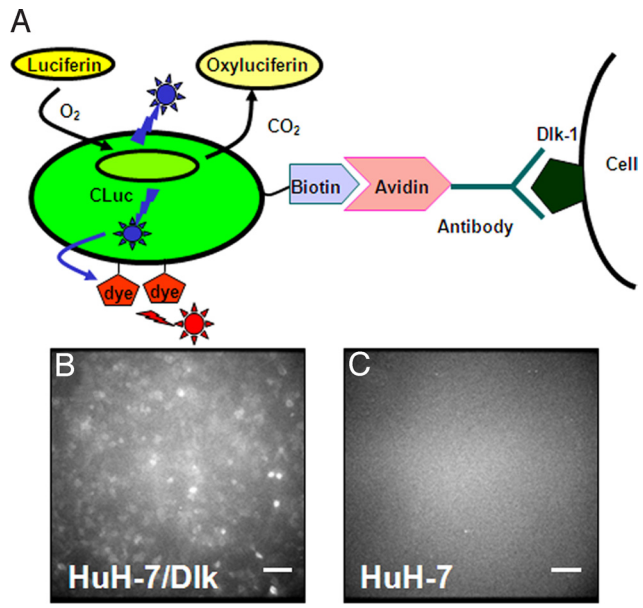


**Fig. 4.** (*A*) Schematic of FBP-IgG showing targeting to tumor cells. (*B*) BLI of Dlk-1-positive Huh-7/Dlk cells. (*C*) BLI of Dlk-1-negative Huh-7 cells. (Scale bars, 200 $\mu$m).

Fluorescence imaging of the mice was performed just before luciferin injection using the same CCD imaging system and a set of Cy-5 filters. Although CLuc-IgG does not contain the fluorescent dye, autofluorescence from tissue was observed (Fig. 5*G*). During the initial 20 min after the injection of FBP-IgG, we observed a strong fluorescent signal from the whole of the animal, because of blood circulation (Fig. 5*H*). However, at 24 h postinjection of the imaging probes, fluorescence images showed little difference between CLuc and FBP of fluorescent signals at tumor sites (Fig. 5 *I* and *J*). In addition, at 48 h postinjection, bioluminescence images and fluorescence images were similar to those seen at 24 h postinjection (Fig. S2 *C–J*).

## Discussion

The use of luciferase as a bioluminescent tag is a convenient and clean approach for in vivo imaging with advantages over radioactivity; also, background is much lower with bioluminescence than with fluorescence. CLuc is a well-known bioluminescent enzyme. Its high quantum yield and turnover-rate makes it a sensitive reporter in small animals as well as in vitro. A limiting factor for the use of CLuc as a bioluminescent tag for in vivo imaging is the blue emission that overlaps with the absorption spectrum of hemoglobin. In the present study, we chose an organic dye as the energy acceptor for BRET with CLuc because of its low molecular weight. The bioluminescence spectrum of CLuc overlaps a part of the absorption spectrum of the dye (Fig. S3). BRET efficiency was estimated to be 0.3, based on the ratio of light intensity at 675 nm to that at 460 nm (Fig. 1*C*). A possible alternative approach would be the use of a luciferase system that emits red light, such as the railroad worm *Phrixothrix*, whose emission peaks at 628 nm, Although we have not evaluated this system, its recombinant luciferase may not be suitable as it is an unstable protein (27). Furthermore its bioluminescent system requires the cofactor ATP, which is not available in extra-cellular environments.

For the detection of liver cancer cells, we prepared a monoclonal antibody against Huh-7 cells expressing Dlk-1. Chemical conjugation of the anti-Dlk-1 antibody to avidin yielded a high molecular weight complex (Fig. 3*A*). We obtained high-resolution microscopic BLI using the avidin-bound unreduced antibody and FBP (Fig. 4*B*), an example of such imaging in single isolated antigen-expressing cells without an external light source. On the other hand, we found that its utility in live animals was poor (Fig. S4). Therefore, we conjugated the reduced antibody to avidin for in vivo imaging, and found that it can be used to target the cell surface antigen despite its low avidity compared to full antibody. Previous studies have shown that fusion of antibody fragments with a luciferase is another efficient way to label antigens on the cell surface (28, 29). However, our chemical conjugation is more easily applicable to the preparation of other CLuc-antibody probes targeting various disease-specific markers, because many antibodies are commercially available.

We found that FBP displayed a 2-fold increase in light output versus CLuc as a bioluminescent tag for in vivo imaging (Fig. 5 *C* and *D*). Since CLuc and FBP use the same luciferase and luciferin, the increased light emission in the far-red part of the spectrum is the direct cause of the improvement of the signal to noise ratio. With fluorescence imaging, we found several difficulties for tumor-specific detection. The images (Fig. 5*G*) show fluorescence signals from the CLuc-IgG mouse because of endogenous fluorophores. In the mouse injected with excess amount of FBP (20 $\mu$g), we found a strong fluorescence signal from the whole body (Fig. 5*H*). However, little difference

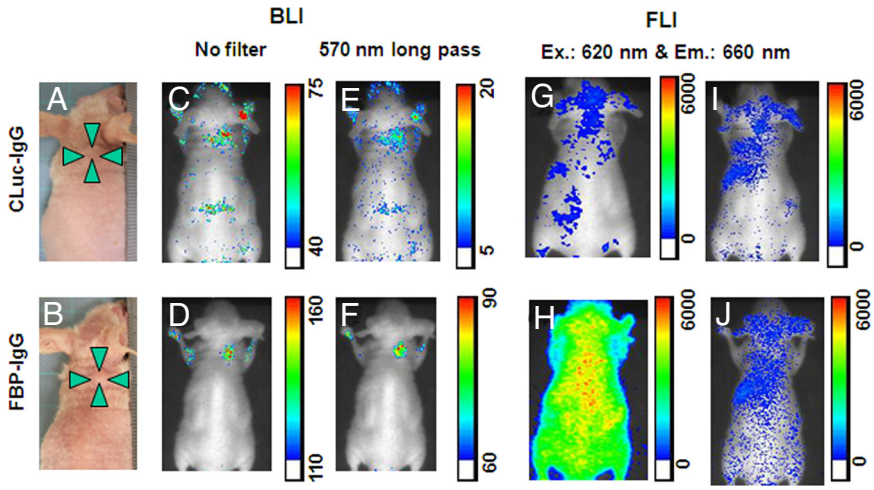


**Fig. 5.** Images of live animals. (*A* and *B*) Photographs of two tumor-bearing mice. (*C* and *D*) 24 h after the administration of CLuc-IgG or FBP-IgG, luciferin was injected and the bioluminescence images (BLIs) were obtained using a CCD photon imaging system. Color scale, photons/s/steradian. (*E* and *F*) The bioluminescence images were obtained with 570 nm long-pass filter. (*G* and *H*) Fluorescence images (FLIs) of tumor-bearing mice shown in panels *A* and *B* immediately after the administration of CLuc-IgG or FBP-IgG were obtained with the same CCD photon imaging system and a set of Cy5 filters. (*I* and *J*) FLIs of the tumor-bearing mice shown in panels *A* and *B* 24 h after administration of CLuc-IgG or FBP-IgG, but before luciferin injection, were obtained under same conditions.

between tumor sites and normal tissues were observed at 24 h (Fig. 5*J*) and 48 h (Fig. S2*J*).

In summary, we have established a bioluminescent protein based on CLuc and a fluorescent dye. This BRET system can be used in the imaging of tumor tissues in small animals. Meanwhile the performance of FBP has been shown to be better than that of CLuc in vivo. Although little is known about the toxicity of *Cypridina* luciferin and *Cypridina* luciferase, and this remains to be investigated, this FBP offers a very useful analytical tool for the evaluations of monoclonal antibody localization in live animals.

## Materials and Methods

**Preparation of FBP.** A mixture of 0.1 mg biotinylated CLuc and 1 $\mu$mol sodium metaperiodate in 0.1 ml of 0.1 M sodium acetate buffer (pH 5.2) was incubated at 4 °C for 30 min. To stop the reaction, glycerol was added to a final concentration of 15 mM. The reaction mixture was incubated at 4 °C for 5 min and then loaded onto a size-exclusion column. Oxidized biotinylated CLuc was eluted with 0.1 M sodium acetate buffer (pH 5.2). Fractions giving strong bioluminescence signals were pooled and concentrated using an Ultrafree-0.5 centrifugal filter device and an equivalent volume of 10 mM HiLyte Fluor™ 647 hydrazide (AnaSpec) in 0.1 M sodium acetate buffer (pH 5.2) was added. The mixture was incubated at room temperature for 2 h, and then loaded onto a size-exclusion column, and FBP was eluted with the 0.1 M potassium phosphate buffer (pH 7.2) containing 0.15 M NaCl. Fractions showing strong bioluminescence signals were combined and stored at 4 °C until use. Bioluminescence emission spectra were measured by mixing 0.1 mM *Cypridina* luciferin and FBP in various buffers on an ATTO AB-1850 LumiFL-Spectrocapture. To determine the effects of pH on the bioluminescence spectra, a 100 mM sodium phosphate buffer (pH 6.5), 100 mM Tris-HCl buffer (pH 7.4) or 100 mM Tris-HCl buffer (pH 8) containing 0.1 M NaCl were used. To determine the effects of high ion concentration on bioluminescence spectra, the same buffers containing 0.5 M NaCl was used, while to determine the effect of hemoglobin on the bioluminescence spectra, 100 mM Tris-HCl buffer containing 0.1 M NaCl and 150 mg/mL hemoglobin was used. All spectra were normalized. Relative light intensity was measured by the addition of Cypridina luciferin (40 ng) to the PBS buffer (100 $\mu$L) or blood (100 $\mu$L) containing either FBP (25 ng) or CLuc (25 ng).

**Isolation of Full-Length Dlk-1 cDNA from Human.** PCR primers were designed based on the gene sequences of human Dlk-1 (GenBank accession no. U15979). Sequences of the prepared primers were as follows: forward primer: 5′-cgc-gtc-cgc-aac-cag-aag-ccc-3′ and reverse primer: 5′-aag-ctt-gat-ctc-ctc-gtc-gcc-ggc-c-3′. To the reverse primer, *Hin*dIII restriction site was added. PCR was performed using these primers and cDNAs synthesized from total RNAs prepared from human liver at embryonic week 10 (TaKaRa). PCR product was cloned into PCRII vector (Invitrogen) (pCRII-hdlk-1). To construct the expression vector, Flag tag sequences were inserted into the *Hin*dIII/*Sal*I site of pBluescript II SK(+) vector (Stratagene) (pBS-Flag). Then, an *Eco*RI/*Hin*dIII fragment was cleaved off from pCRII-hdlk-1 and inserted into the *Eco*RI/*Hin*dIII site of pBS-Flag vector (pBS-hdlk-1-Flag). An *Eco*RI/*Sal*I fragment was cleaved off from pBS-hdlk-1-Flag and inserted into the *Eco*RI/*Xho*I site of pcDNA3.1 vector (Invitrogen) (pcDNA-hdlk-1-Flag).

**Generation of Cell Lines Stably Expressing Dlk-1.** The HEK293 cell and Huh-7 cell line derived from human liver cancer were furnished by the Japan Health Sciences Foundation. The expression vector pcDNA-hdlk-1-Flag was introduced into those cell lines using LipofectAMINE-plus reagent (Invitrogen), in accordance with the manufacturer's instruction. After selection with G418 antibiotic (Geneticin, Calbiochem), the HEK293-hdlk-1 and the Huh-7-hdlk-1 cell line that stably expresses human Dlk-1 were established.

**Generation of Anti-Dlk-1 Monoclonal Antibody.** Mice (BALB/c) were immunized with HEK293 cells that stably express human Dlk-1 or with the expression vector that encodes full-length human Dlk-1 cDNA. Hybridomas were generated by fusion of B cells to mouse myeloma cells (P3-X63-Ag8.653 or SP2/0-Ag14) by a conventional method. After selection with HAT supplement (Invitrogen) containing media, hybridoma clones each of which produces an anti-human Dlk-1 monoclonal antibody were screened by ELISA and flow cytometry. To prepare purified antibody protein, the hybridoma clone was i.p. administered to BALB/c nude mice at a dose of $3 \times 10^6$ cells, which was treated with 2,6,10,14-tetramethylpentadecane (pristane) 7 days before administration. After collection of ascites, the monoclonal antibody (DI-2–20) was purified with a protein G column (GE Healthcare).

**Immunostaining and Western Blot Analyses.** For immunocytostaining, Huh-7/Dlk and Huh-7 cells were cultured and fixed with ice-cold 100% methanol. Hoechst33342 was used for nuclear staining. Newly developed anti-human Dlk-1 monoclonal antibody (DI-2–20) and a goat FITC-labeled anti-mouse IgG (Santa Cruz Biotechnology) were used for Dlk-staining. For western blot analysis, Huh-7/Dlk and Huh-7 cells were harvested and whole cell protein extracts were prepared. Thirty $\mu$g protein was separated by 10% SDS/PAGE and transferred to a nitrocellulose membrane. An anti-human Dlk-1 monoclonal antibody (DI-2–20) and goat anti-mouse IgG (Santa Cruz Biotechnology) were used as primary and secondary antibodies, respectively.

**Avidin Antibody.** Conjugation of anti-human Dlk-1 monoclonal antibody or reduced antibody to avidin was performed with EZ-link maleimide activated NeutrAvidin™ protein, in accordance with the manufacturer's instruction (Pierce). The avidin-bound antibody was purified by gel filtration column chromatography using a TSK gel G3000SW column (Tosoh). Collected fractions were diluted and then added to a 96-well plate precoated with goat anti-mouse IgG. After the plate was washed, a solution of FPB was added and

incubation was carried out. Bioluminescent measurements were performed with a 96-well plate reader (Berthold Technologies) after adding of 100 $\mu$L of 1 $\mu$M Cypridina luciferin solution (0.1 M Tris-HCl pH7.4/0.3 M sodium ascorbate/0.02 M sodium sulfite) to each well.

**Living-Cell BLI.** For live-cell BLI, Huh-7/Dlk and Huh-7 cells were cultured and washed with cold PBS buffer containing 1% BSA (1% BSA/PBS). Each cell line was incubated with the probe solution containing avidin-bound antibody (25 $\mu$g) and FBP (25 $\mu$g), diluted with 1% BSA/PBS buffer at 4 °C for 120 min, and then washed three times with 1% BSA/PBS buffer. PBS buffer containing *Cypridina* luciferin (1 $\mu$M) was added to detect luminescence from the probes on the cell surface. Light was measured with Cellgraph™ (ATTO Co.) with 5-min exposure.

**Optical Imaging in Live Animals.** Six-week-old male BALB/c nu/nu mice each weighing ≈20 g were obtained from CLEA Japan, Inc.). All procedures involving animals and their care were approved by the Ethics Committee of Hokkaido University in accordance with institutional and Japanese government guidelines for animal experiments. Huh-7/Dlk cells ($5 \times 10^6$ cells/animal) in 100 $\mu$L solution (PBS: Matrigel = 1: 1) were implanted s.c. into the back of mice. Matrigel was obtained from BD Biosciences. Tumor growth was monitored until it reached an acceptable size. For in vivo imaging, a 0.8-mL solution containing FBP-IgG or CLuc-IgG (25 ng/$\mu$L) was injected to mice intravenously. The same experiments were carried out twice. To obtain bioluminescence image, the mice were given injections of 100 $\mu$L of 2 $\mu$g/$\mu$L *Cypridina* luciferin at 24 h or 48 h. Bioluminescence imaging was performed by Photon Imager (Biospace Lab) equipped with an intensified CCD camera (18 mm diameter, objective lens: 24 mm, f/1.4–22) between 5 and 10 min after luciferin injection with 0.5-min exposure in the absence or in the presence of 570 nm long pass filter (30). In vivo fluorescence imaging was carried out just before luciferin injection using the same equipment with a Cy5 filter set (a 60-nanometer excitation pass band filter from 590 to 650 nanometers with a peak at 620 nm, and a 660 nanometers long-pass filter for the detection of emission) with 0.5-min exposure.

**ACKNOWLEDGMENTS.** This study was supported in part by a Grant-in-Aid for the Support of Young Researchers (grant no. 19710196 to C.W.), Grant-in-Aid (A) (grant no. 20249060 to M.O.) and Grant-in-Aid (C) (grant no. 19614002 to Y.O.) from the Ministry of Education, Culture, Sports, Science, and Technology, Japan. We thank Dr. S. Ohgiya (AIST) for his comments on the manuscript.

1. Adams R, Meade A, Wasan H, Griffiths G, Maughan T (2008) Cetuximab therapy in first-line metastatic colorectal cancer and intermittent palliative chemotherapy: Review of the COIN trial. *Expert Rev Anticancer Ther* 8:1237–1245.
2. Boltze J, et al. (2008) Permanent middle cerebral artery occlusion in sheep: A novel large animal model of focal cerebral ischemia. *J Cereb Blood Flow Metab* 28:1951–1964.
3. Ilowite NT (2008) Update on biologics in juvenile idiopathic arthritis. *Curr Opin Rheumatol* 20:613–618.
4. Menard C, et al. (2008) Ctla-4 blockade confers lymphocyte resistance to regulatory T-cells in advanced melanoma: Surrogate marker of efficacy of tremelimumab? *Clin* Cancer Res 14:5242–5249.
5. Wang Z, et al. (2008) Effect of rapamycin alone and in combination with sorafenib in an orthotopic model of human hepatocellular carcinoma. *Clin Cancer Res* 14:5124–5130.
6. Contag PR, Olomu IN, Stevenson DK, Contag CH (1998) Bioluminescent indicators in living mammals. *Nat Med* 4:245–247.
7. Hoffman RM, Yang M (2005) Dual-color, whole-body imaging in mice. *Nat Biotechnol* 23:790.
8. Ntziachristos V, Ripoll J, Wang LV, Weissleder R (2005) Looking and listening to light: The evolution of whole-body photonic imaging. *Nat Biotechnol* 23:313–320.
9. So MK, Xu C, Loening AM, Gambhir SS, Rao J (2006) Self-illuminating quantum dot conjugates for in vivo imaging. *Nat Biotechnol* 24:339–343.
10. Frangioni JV (2006) Self-illuminating quantum dots light the way. *Nat Biotechnol* 24:326–328.
11. Xu Y, Piston DW, Johnson CH (1999) A bioluminescence resonance energy transfer (BRET) system: Application to interacting circadian clock proteins. *Proc Natl Acad Sci USA* 96:151–156.
12. Shcherbo D, et al. (2007) Bright far-red fluorescent protein for whole-body imaging. *Nat Methods* 4:741–746.
13. Frangioni JV (2003) In vivo near-infrared fluorescence imaging. *Curr Opin Chem Biol* 7:626–634.
14. Shimomura O, Johnson FH (1971) Mechanism of the luminescent oxidation of *Cypridina* luciferin. *Biochem Biophys Res Commun* 44:340–346.
15. Thompson EM, Nagata S, Tsuji FI (1989) Cloning and expression of cDNA for the luciferase from the marine ostracod *Vargula hilgendorfii*. *Proc Natl Acad Sci USA* 86:6567–6571.
16. Nakajima Y, Kobayashi K, Yamagishi K, Enomoto T, Ohmiya Y (2004) cDNA cloning and characterization of a secreted luciferase from the luminous Japanese ostracod, *Cypridina noctiluca*. *Biosci Biotechnol Biochem* 68:565–570.
17. Shimomura O, Johnson FH, Saiga Y (1961) Purification and properties of *Cypridina* luciferase. *J Cell Comp Physiol* 58:113–123.
18. Shimomura O, Johnson FH, Masugi T (1969) *Cypridina* bioluminescence: Light-emitting oxyluciferin-luciferase complex. *Science* 164:1299–1300.
19. Wu C, et al. (2007) Preparation of biotinylated *Cypridina* luciferase and its use in bioluminescent enzyme immunoassay. *Anal Chem* 79:1634–1638.
20. Wu C, Kawasaki K, Ohgiya S, Ohmiya Y (2006) Syntheses and evaluation of the bioluminescent activity of (S)-*Cypridina* luciferin and its analogs. (Translated from English) *Tetrahedron Lett* 47:753–756.
21. Laborda J, Sausville EA, Hoffman T, Notario V (1993) dlk, a putative mammalian homeotic gene differentially expressed in small cell lung carcinoma and neuroendocrine tumor cell line. *J Biol Chem* 268:3817–3820.
22. Kogel D, et al. (2001) Dlk/ZIP kinase-induced apoptosis in human medulloblastoma cells: Requirement of the mitochondrial apoptosis pathway. *Br J Cancer* 85:1801–1808.
23. Tanimizu N, Nishikawa M, Saito H, Tsujimura T, Miyajima A (2003) Isolation of hepatoblasts based on the expression of Dlk/Pref-1. *J Cell Sci* 116:1775–1786.
24. Hsiao CC, et al. (2005) Differential expression of delta-like gene and protein in neuroblastoma, ganglioneuroblastoma and ganglioneuroma. *Mod Pathol* 18:656–662.
25. Dezso K, et al. (2008) Delta-like protein (DLK) is a novel immunohistochemical marker for human hepatoblastomas. *Virchows Arch* 452:443–448.
26. Schatz PJ (1993) Use of peptide libraries to map the substrate specificity of a peptide-modifying enzyme: A 13-residue consensus peptide specifies biotinylation in Escherichia coli. *Biotechnology* 11:1138–1143.
27. Nakajima Y, Kimura T, Suzuki C, Ohmiya Y (2004) Improved expression of novel red- and green-emitting luciferases of *Phrixothrix* railroad worms in mammalian cells. *Biosci Biotechnol Biochem* 68:948–951.
28. Venisnik KM, et al. (2006) Bifunctional antibody-*Renilla* luciferase fusion protein for in vivo optical detection of tumors. *Protein Eng Des Sel* 19:453–460.
29. Venisnik KM, Olafsen T, Gambhir SS, Wu AM (2007) Fusion of *Gaussia* luciferase to an engineered anti-carcinoembryonic antigen (CEA) antibody for in vivo optical imaging. *Mol Imaging Biol* 9:267–277.
30. Roncali E, et al. (2008) New device for real-time bioluminescence imaging in moving rodents. *J Biomed Opt* 13:054035.